Phase transitions in two-dimensional uniformly frustrated XY spin systems

B. Berge* and H. T. Diep
Laboratoire de Magnétisme des Surfaces, Université de Paris VII, 2 place Jussieu, 75251 Paris Cédex 05, France

A. Ghazali
Groupe de Physique des Solides de l'Ecole Normale Supérieure, Université de Paris VII, 2 place Jussieu, 75251 Paris Cédex 05, France

P. Lallemand
Laboratoire de Spectroscopie Hertzienne de l'Ecole Normale Supérieure, Université Pierre et Marie Curie (Paris VI), 24 rue Lhomond, 75231 Paris Cédex 05, France

(Received 12 July 1985)

We investigate the nature of phase transitions in a generalized uniformly frustrated square-lattice model with XY spins. The frustration is made to vary by changing the negative bond strength η. From ground-state (GS) analysis we find that, below the critical value $\eta=\frac{1}{3}$, the GS is ferromagnetic, while for $\eta>\frac{1}{3}$, it is doubly degenerate with canted spin configurations. This suggests the existence of an Ising-like transition. This is confirmed by our extensive Monte Carlo simulations. In addition, there is a Kosterlitz-Thouless-like transition at higher temperature for $\eta\neq 1$. In the fully frustrated case ($\eta=1$), these two transitions are merged into a single one of dominant Ising character. These conclusions follow from a finite-size-scaling analysis and a visualization of the ordering.

I. INTRODUCTION

The concept of frustration was initially introduced in connection with spin glasses.[1] Since then, frustration effects have been widely investigated not only in spin glasses but also in uniformly frustrated systems without disorder. The latter systems are periodically defined, so they are potentially amenable to exact treatment and can serve as testing grounds for various statistical theories and approximations. Experimentally, some real systems such as planar arrays of Josephson junctions in transverse magnetic fields and fcc alloys can already be modeled by uniformly frustrated systems. Other examples can be found in topics such as incommensurate surface reconstructions and ^{3}He-A films (see, e.g., papers cited in Ref. 2).

Uniformly frustrated three-dimensional (3D) systems studied so far present rich and often unexpected behavior. For example, in the fully frustrated simple-cubic lattice with Ising spins, a second-order transition has been found and a partial disorder occurs in the ordered phase.[3] The same features have also been observed in a stacked antiferromagnetic triangular lattice with Ising spins.[4,5] The antiferromagnetic fcc lattice with Ising spins, on the other hand, possesses a first-order transition.[6,7] In a partially frustrated 3D Ising system, evidence of linear-chain-like excitations has been found.[8] In addition, interesting and unexpected ground-state (GS) properties of the fully frustrated simple-cubic lattice with vector spins have been discovered very recently.[9,10]

In 2D systems, Villain's fully frustrated model[11] (see Fig. 1) and the antiferromagnetic triangular lattice,[12] while presenting no finite-temperature transition for Ising spins in agreement with Monte Carlo (MC) simulations,[13,4,5] show a phase transition at finite temperature for XY spins as obtained by MC simulations (see Ref. 14 for Villain's model and Refs. 15 and 16 for the triangular lattice). However, the nature of the phase transition in these two systems with XY spins is not well understood, though it has been suggested[14–18] that the phase transition has a somewhat mixed character, of both Kosterlitz-Thouless[19] (KT) type and Ising type. This suggestion is based on the fact that the GS degeneracy in both square[11] and triangular[15,16] systems is twofold in addition to the degeneracy due to global rotation of the spin system. The first kind of degeneracy yields an Ising-like transition

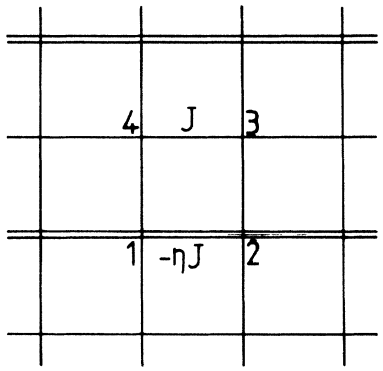

FIG. 1. Uniformly frustrated square lattice: single lines are positive bonds ($J>0$) and double lines represent bonds which are equal to $-\eta J$. The Villain model corresponds to $\eta=1$. The spins on a plaquette are numbered for ground-state analysis.

where the disorder arises from random mixing of two degenerate states, while the second kind gives rise to the KT-type transition initially predicted for 2D ferromagnetic XY systems.[19] These transitions thus correspond to two different kinds of symmetry breaking. The question of how they actually occur, i.e., at the same temperature or one just after the other, has not been clarified so far, either in MC simulations,[14–16] or in Landau-Ginzburg-Wilson analysis.[16–18] This is the motivation behind the present work.

The purpose of this paper is to study in detail the nature of the phase transition in the 2D uniformly frustrated lattice shown in Fig. 1, with classical XY spins. To this end, we make a ground-state analysis and perform extensive MC simulations. Since it is difficult to analyze MC data in the critical region to see if there is a single transition with a double character or two separate transitions (in this case, the question is which one occurs first), we vary the strength of negative bonds (Fig. 1). In doing so, we modify the frustration, expecting that it will split off the transitions far enough from each other, so that one can study the nature of each transition more easily. As it turns out, we have succeeded in making one transition move downwards and the other upwards on the temperature scale. From our data analysis, the low-temperature transition corresponds to an Ising-type transition and the high-temperature one to a KT-type one. Therefore, in the fully frustrated (equal bond strengths) model, our results suggest that if there were two separate transitions, then the low-temperature one would be of Ising type and the high-temperature one of KT type. This at least rules out the possibility[15] that the KT transition occurs first. However, our results strongly favor the existence of a single transition with a double character in this case.

In Sec. II, the GS spin configurations are derived analytically in the general case. We show that there exists a critical strength of negative bonds below which the GS spin configuration becomes ferromagnetic: in this case, the Ising-type transition would disappear since there is no longer twofold degeneracy. This prediction is indeed confirmed by our MC results shown in Sec. III, where finite-size-scaling analysis is also presented. Concluding remarks are given in Sec. IV.

II. GROUND STATE

We consider the model system described by the following Hamiltonian:

$$H=-\sum_{(ij)} J_{ij}\mathbf{S}_i\cdot\mathbf{S}_j \ , \tag{1}$$

where the nearest-neighbor interaction J_{ij} is equal to J for positive bonds which are represented by single lines in Fig. 1, and to $-\eta J$ for bonds which are represented by double lines. The value of η is made to vary from -1 to infinity: $\eta=1$ corresponds to the fully frustrated case while $\eta=-1$ corresponds to the ferromagnetic case. The spins $\mathbf{S}_i$ are planar spins of unit length.

For GS configuration analysis, it suffices to consider just a single plaquette; this will be justified later. Furthermore, we consider as a single solution all configurations obtained from each other by any global spin rotation. For convenience, the spins are numbered as in Fig. 1. The Hamiltonian for the plaquette H_p is written as

$$H_p=\eta\mathbf{S}_1\cdot\mathbf{S}_2-\mathbf{S}_2\cdot\mathbf{S}_3-\mathbf{S}_3\cdot\mathbf{S}_4-\mathbf{S}_4\cdot\mathbf{S}_1 \ . \tag{2}$$

Here, and in what follows, J is taken as a unit of energy. The GS spin configurations are obtained by minimizing H_p with respect to $\mathbf{S}_i$, taking into account the conditions

$$(\mathbf{S}_i)^2=1, \quad i=1,\ldots,4 \ . \tag{3}$$

The variational equation reads

$$\delta\left[H_p-\tfrac{1}{2}\sum_{i=1}^{4}\lambda_i(\mathbf{S}_i)^2\right]=0 \ . \tag{4}$$

Equation (4) amounts to requiring that each spin be aligned along its local field. Now, by symmetry, sites 1 and 2 are equivalent; so are sites 3 and 4. Thus, the Lagrange multipliers λ_1 and λ_2 are equal; so are λ_3 and λ_4. Note that the local fields are nothing but absolute values of the multipliers $\lambda=\lambda_1=\lambda_2$ and $\mu=\lambda_3=\lambda_4$. Equation (4) leads to the following set of equations:

$$\begin{aligned}
&\lambda\mathbf{S}_1-\eta\mathbf{S}_2+\mathbf{S}_4=0 \ , \\
&-\eta\mathbf{S}_1+\lambda\mathbf{S}_2+\mathbf{S}_3=0 \ , \\
&\mathbf{S}_2+\mu\mathbf{S}_3+\mathbf{S}_4=0 \ , \\
&\mathbf{S}_1+\mathbf{S}_3+\mu\mathbf{S}_4=0 \ .
\end{aligned} \tag{5}$$

In fact, from (5) one obtains two decoupled homogeneous sets of equations:

$$\begin{aligned}
&(\lambda-\eta)(\mathbf{S}_1+\mathbf{S}_2)+(\mathbf{S}_3+\mathbf{S}_4)=0 \ , \\
&(\mathbf{S}_1+\mathbf{S}_2)+(\mu+1)(\mathbf{S}_3+\mathbf{S}_4)=0
\end{aligned} \tag{6a}$$

and

$$\begin{aligned}
&(\lambda+\eta)(\mathbf{S}_1-\mathbf{S}_2)+(\mathbf{S}_4-\mathbf{S}_3)=0 \ , \\
&(\mathbf{S}_1-\mathbf{S}_2)+(\mu-1)(\mathbf{S}_4-\mathbf{S}_3)=0 \ .
\end{aligned} \tag{6b}$$

Equations (6) yield

$$\mu=-\left[\frac{1+\eta}{\eta}\right]^{1/2} , \tag{7a}$$

$$\lambda=\eta\mu=-[\eta(1+\eta)]^{1/2} \ . \tag{7b}$$

To obtain the angle between two spins, e.g., $\mathbf{S}_1$ and $\mathbf{S}_4$, one rewrites the first equation of (5) as

$$(\lambda\mathbf{S}_1+\mathbf{S}_4)^2=(-\eta\mathbf{S}_2)^2 \ .$$

This gives

$$\mathbf{S}_1\cdot\mathbf{S}_4=\frac{1}{2\lambda}(\eta^2-\lambda^2-1)=\frac{1}{2}\left[\frac{\eta+1}{\eta}\right]^{1/2} .$$

In the same way, one sees that the cosines of the angles θ_{ij} of the spins $\mathbf{S}_i$ and $\mathbf{S}_j$ linked by positive bonds are all equal and given by

$$\cos\theta=\cos\theta_{23}=\cos\theta_{34}=\cos\theta_{41}=\frac{1}{2}\left[\frac{\eta+1}{\eta}\right]^{1/2} . \tag{8a}$$

Moreover,

$$|\theta_{12}| = 3|\theta| \ , \tag{8b}$$

$$|\theta_{13}| = |\theta_{24}| = 2|\theta| \ . \tag{8c}$$

Now, since the cosines in (8a) never exceed one, we are led to a lower critical value of η, namely,

$$\eta = \tfrac{1}{3} \ , \tag{9}$$

below which there is only one GS spin configuration, the ferromagnetic one. For $\eta > \frac{1}{3}$, the spin configuration is canted. As seen from (8a), the angle between adjacent spins on positive bonds varies continuously from zero for $\eta \leq \frac{1}{3}$ to either $\pi/3$ or $-\pi/3$ for infinite η: there is a bifurcation of the ferromagnetic solution toward the two canted solutions at $\eta = \frac{1}{3}$. The degeneracy in this case is easily seen: given the orientation of, say, $\mathbf{S}_2$, there are only two possible orientations for $\mathbf{S}_3$, according to (8a). Once the orientation of $\mathbf{S}_3$ is chosen, the orientations of the remaining spins are determined. Furthermore, the remaining spins of the adjacent plaquettes are also determined; in this way, the GS spin configuration of the whole system is determined. Thus, the GS in the case $\eta > \frac{1}{3}$ is doubly degenerate. This generalizes the well-known result for the fully frustrated case ($\eta = 1$).[11]

As long as the double degeneracy exists (i.e., $\eta > \frac{1}{3}$), one should expect one transition of Ising type. This is indeed confirmed by the results of MC simulations given in the following section.

In the GS, the energy of each plaquette is minimized, therefore, the GS energy of the system is given by one-half of the sum of the plaquette energies. This justifies the use of a single plaquette to look for GS spin configurations. The GS energy per spin is easily found to be

$$U_0 = -\frac{3-\eta}{2} \quad \text{for } \eta < \tfrac{1}{3} \ , \tag{10a}$$

$$U_0 = -\frac{1}{2}\frac{(1+\eta)^{3/2}}{\eta^{1/2}} \quad \text{for } \eta > \tfrac{1}{3} \ . \tag{10b}$$

We note that both U_0 and $dU_0/d\eta$ are continuous for $\eta = \frac{1}{3}$. In addition, U_0 presents a flat maximum at $\eta = \frac{1}{2}$. The GS magnetization modulus per spin is given by

$$m = \tfrac{1}{2}\cos\theta[2(1+\cos\theta)]^{1/2} \ . \tag{11}$$

III. MONTE CARLO SIMULATIONS AND INTERPRETATION OF RESULTS

The MC procedure we use here has been described in detail elsewhere.[9] We have used the sample sizes of $L^2 = 20^2$, 30^2, 40^2, 50^2, 70^2, and 100^2 spins for various values of η. The large sizes have been used only for finite-size-scaling analysis in the critical regions. Periodic boundary conditions have been used. In addition, one of the GS spin configurations has been taken as an initial spin configuration since initial random spin configurations often lead to wall defects at low temperatures. In each run, we have discarded about 20 000 MC steps per spin before averaging physical quantities over the next 50 000 MC steps per spin. We note that in each run the number of MC steps per spin given here is the total number of flippings per spin.

A. Energy and specific heat

In Fig. 2, internal energy per spin U is plotted as a function of temperature T for different values of η. For the fully frustrated system ($\eta = 1$), one observes a sharp change of curvature of U. In the inset, the size effect on U in the critical region is shown: one cannot exclude the possibility of a weak first-order transition. For η different from 1 but larger than $\frac{1}{3}$, there are two downward curvatures of U in contrast with the case $\eta = 1$. This suggests the existence of two transitions.

The specific heat per spin C obtained by differentiating U with respect to T is shown as a function of T in Fig. 3 for different values of η. For η far enough from 1 but larger than $\frac{1}{3}$, one clearly observes two distinct peaks. The low-temperature peak is sharp and the high-temperature one is rounded even for sizes as large as 100^2. As can be seen from Fig. 3, when η approaches 1 from below and above, the two peaks are merged into a single peak.

In order to investigate the nature of the transitions associated with the peaks of C, we have made a careful finite-size-scaling analysis of the peak heights of specific heat $C_{\max}$ and inspected snapshots of the spin system in different temperature regions. Other quantities have also been examined.

In the case where two peaks exist in C, we show, respectively, in Figs. 4(a) and 4(b), the low- and high-temperature peak heights $C_{\max}$ as functions of $\ln L$. The low-temperature peak height increases linearly with $\ln L$. This indicates a critical exponent $\alpha = 0$ which is characteristic of the Ising transition. The logarithmic dependence of C on the temperature has been checked on both

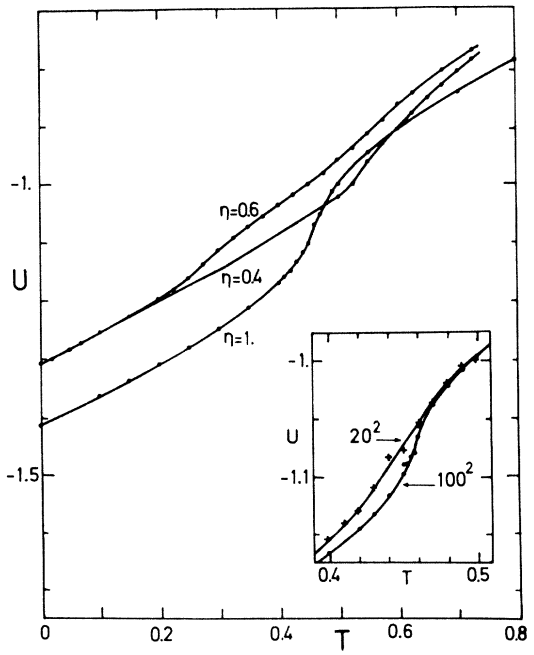

FIG. 2. Internal energy per spin U as a function of temperature T, for various values of η, with $L^2 = 30^2$. The finite-size effect in the critical region in the $\eta = 1$ case is shown in the inset.

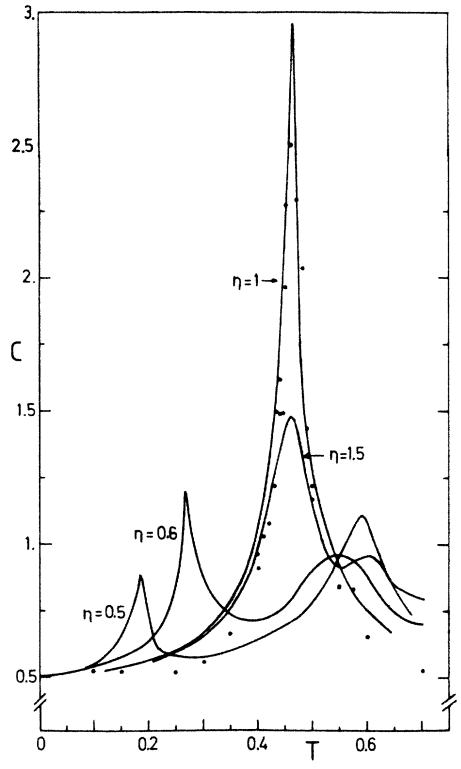

FIG. 3. Specific heat per spin C, obtained by differentiating U with respect to temperature T, is shown as a function of T, for various values of η ($L^2=30^2$). Results obtained by energy fluctuations (solid circles) are shown for $\eta=1$.

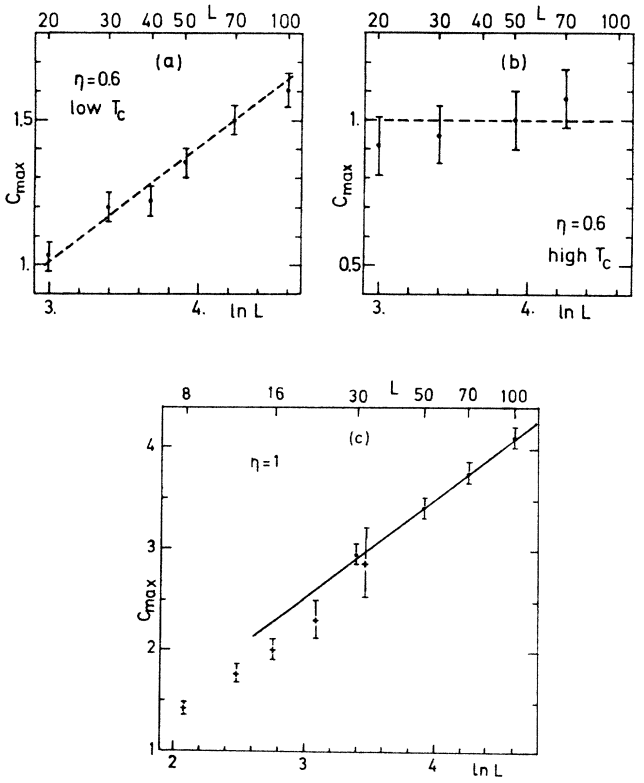

FIG. 4. Finite-size scaling of peak height C_{max} of specific heat: (a) for the low-temperature transition with $\eta=0.6$; (b) for the high-temperature transition with $\eta=0.6$; (c) for the single transition with $\eta=1$. The results of Ref. 14 for small lattice sizes are reproduced here (crosses).

sides of the transition. The Ising character will be further confirmed by a visualization method presented below. On the other hand, the high-temperature C_{max} is independent of L for large enough L [see Fig. 4(b)]; this is a characteristic feature of the KT transition as also numerically observed in ferromagnetic XY model.[20,21]

We note that Lee *et al.*[16] have obtained two transitions for an antiferromagnetic XY model on a triangular lattice in the presence of a magnetic field. The low and high transitions correspond, respectively, to Ising-like and KT-like transitions. They have interpreted the latter as a result of the screening of the vortex interaction by solitons (domain walls).

In the fully frustrated case ($\eta=1$), the peak in C is very sharp (see Fig. 3). The peak height C_{max} increases linearly with $\ln L$ as shown in Fig. 4(c), where data of Teitel and Jayaprakash[14] for smaller lattice sizes are also presented. As can be seen, their data exhibit approximately the same slope as ours. Again, we have found a logarithmic temperature dependence of C on both sides of the transition. These results strongly indicate the Ising character of the transition. However, as seen above, this single peak results, in fact, from the superposition of two peaks, the Ising and KT ones. Therefore, the KT character of the transition should also persist at $\eta=1$, although it is hidden by the Ising behavior of C.

If the mechanism proposed by Lee *et al.*[16] is correct, solitons may not screen the vortex interaction enough that the two transitions occur at the same temperature for $\eta=1$.

B. Visualization of ordering

We now examine the spin configuration obtained at the end of the MC run in different temperature regions. Since the spin configuration is canted, it is difficult to visualize the nature of spin ordering. Therefore, we use a projection procedure. We consider a sublattice of plaquettes with periodicity twice the lattice constant. We associate to this sublattice four spin configurations: two GS configurations determined in the preceding section and two obtained from these by a rotation of $\pi/2$. Next, we project the spin configuration of each plaquette (of the same sublattice of plaquettes) obtained by MC simulation on the above four states. Thus we obtain, respectively, four components q_{1x}, q_{2x}, q_{1y}, and q_{2y} which define two vectors $\mathbf{q}_1$ and $\mathbf{q}_2$. If the spin configuration on a plaquette belongs to the first GS, then $|\mathbf{q}_1|=1$ and $|\mathbf{q}_2|=0$, independently of the global spin rotation. If it belongs to the second GS, then $|\mathbf{q}_1|=0$ and $|\mathbf{q}_2|=1$. For an excited plaquette, one has a mixed state ($|\mathbf{q}_1|\neq 0$ and $|\mathbf{q}_2|\neq 0$). Furthermore, a global spin rotation on the pla-

quette corresponds to a rotation of $\mathbf{q}_1$ and $\mathbf{q}_2$ with the same angle. So, the breaking of continuous symmetry which results in an orientational order can be seen by looking at relative orientations of $\mathbf{q}_1$ and $\mathbf{q}_2$ over the entire system.

In Figs. 5(a) and 5(b), we show a map of $\mathbf{q}_1$ and $\mathbf{q}_2$, taken from a portion of the spin system, with $\eta=0.5$, below and above the low-temperature transition, respectively. In Fig. 5(a), there is only one kind of GS ($|\mathbf{q}_1|\simeq 1$ and $|\mathbf{q}_2|\simeq 0$) while in Fig. 5(b), there is a random mixing of clusters of dominant $\mathbf{q}_1$ or $\mathbf{q}_2$ kind. This further confirms the Ising nature of the transition. Note, however, that orientational order still remains after this transition. We do not show here a map of $\mathbf{q}_1$ and $\mathbf{q}_2$ above the high-temperature transition, since orientational disorder occurs rather gradually through the transition region. This is not surprising since the specific heat presents a broad maximum.

For the fully frustrated case ($\eta=1$), a map of $\mathbf{q}_1$ and $\mathbf{q}_2$ below and above the transition is shown in Figs. 6(a) and 6(b), respectively. Again, below the transition, only one kind of GS is observed. Above the transition, not only Ising disorder is present but orientational (KT) disorder is observed as well. This is what one should expect, given the sharp nature of the transition.

C. Phase diagram

Now, we display in Fig. 7, the locus of the peak temperature of C as a function of the frustration parameter η. In the (T,η) plane, the low-temperature branch (dashed curve) represents the Ising-type transition line. Further-

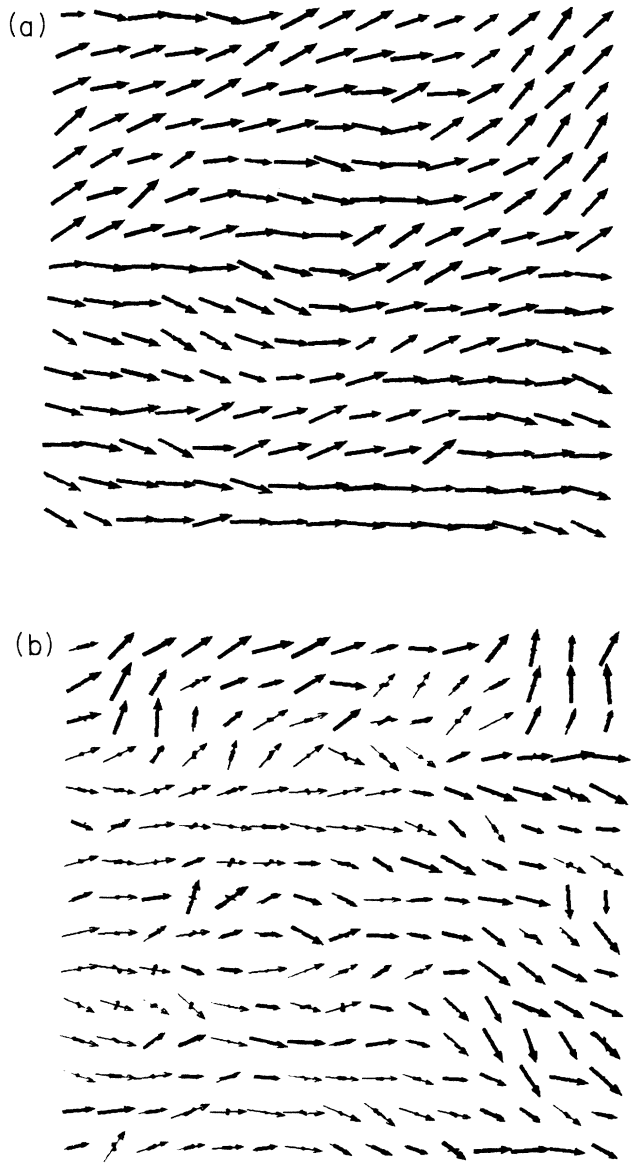

FIG. 5. Map of $\mathbf{q}_1$ and $\mathbf{q}_2$ (see text), represented by thick and thin vectors, respectively, taken from a portion of the system with $\eta=0.5$; (a) at $T=0.1$ (below the low-temperature transition); (b) at $T=0.2$ (between two transitions).

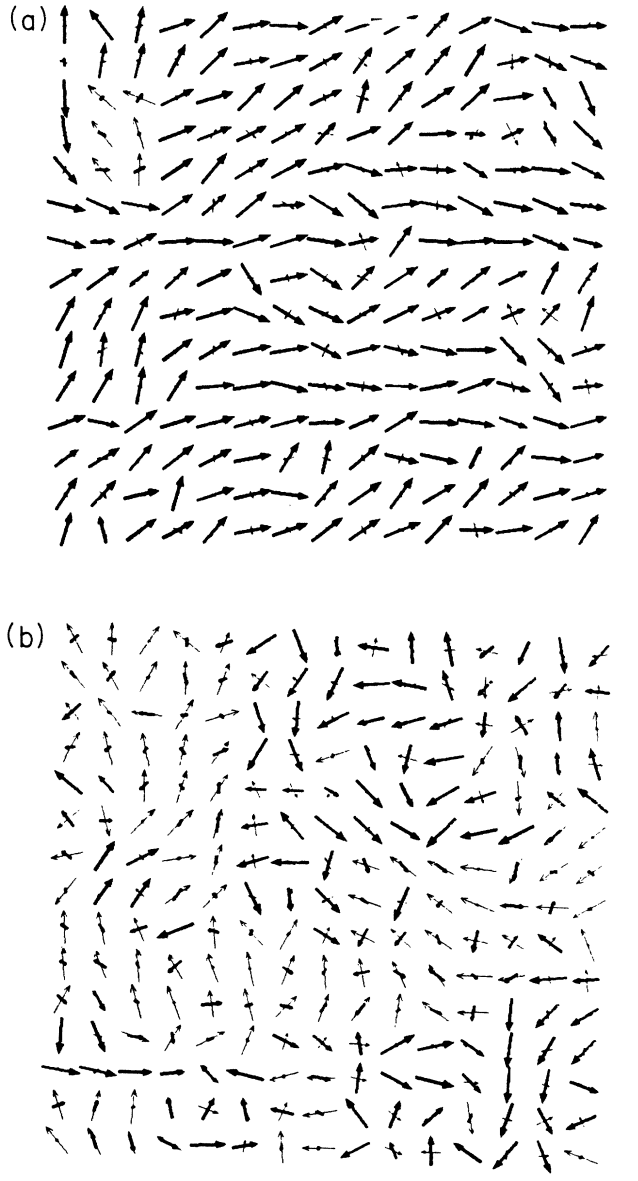

FIG. 6. Map of $\mathbf{q}_1$ and $\mathbf{q}_2$ (thick and thin vectors, respectively) for a portion of the system with $\eta=1$: (a) at $T=0.4$ (below the transition); (b) at $T=0.5$ (above the transition). See text for comments.

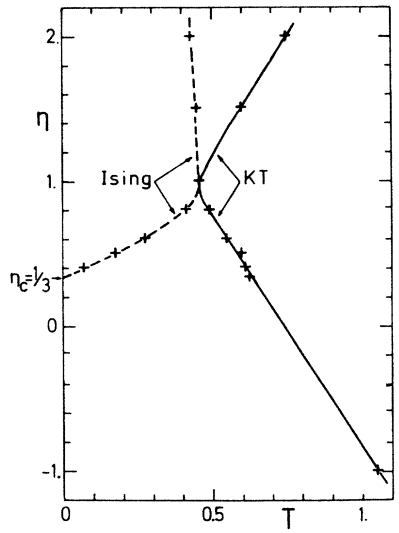

FIG. 7. Phase diagram in the plane (T,η) determined from the locus of the peak temperatures of C. Solid and dashed curves represent the Ising-like and KT-like transition lines respectively.

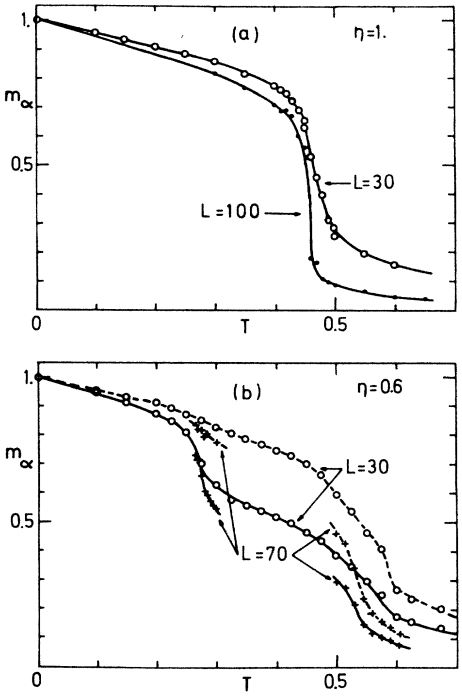

FIG. 8. Sublattice magnetization modulus per spin m_α as a function of temperature for $L^2=30^2$ (open circles). Results for $L^2=70^2$ (crosses) and 100^2 (solid circles) in the critical regions are shown to appreciate finite-size effect: (a) $\eta=1$; (b) $\eta=0.6$. Solid lines are for sublattices 1 and 2; dashed lines are for sublattices 3 and 4.

more, the high-temperature branch (solid curve) represents provisionally the KT-type transition line, since it is known, at least in the XY ferromagnetic case,[20,21] that the locus of specific-heat maxima does not coincide with the KT transition points. So, in what follows, when we mention the KT-type transition line, we mean only the locus of specific-heat maxima. Note, however, that this locus coincides with that of magnetic-susceptibility maxima for $\eta \leq 1$ (see Sec. III E). Note that in the vicinity of $\eta=1$, it was not possible to resolve the peaks of C, so the phase diagram in this region should be read qualitatively. It is interesting to note that for $\eta>1$, the Ising-type transition temperature is almost independent of η. This indicates that the energy barrier between the two degenerate states is insensitive to varying η. This may be understood from the following argument: the energy barrier is a function of θ which is itself a slowly varying function of η for large η [Eq. (8a)]. On the other hand, the KT-type transition temperature is almost a linear function of η for large positive or negative η as one should expect since the orientational ordering is then controlled by the η bonds.

D. Sublattice magnetizations and correlation functions

We show in Figs. 8(a) and 8(b), sublattice magnetization moduli per spin as functions of temperature for $\eta=1$ and 0.6, respectively. The magnetization modulus per spin m_α of sublattice α is defined by

$$m_\alpha=\frac{4}{L^2}\left\langle \left| \sum_{i\in\alpha} \mathbf{S}_i \right| \right\rangle , \tag{12}$$

where the angular brackets indicate the thermal average. By this definition, one gets rid of the global spin rotation in the long-time average. For $\eta=1$, all sublattice magnetization moduli are equal; one observes a sharp fall of m_α at the transition temperature. For $\eta=0.6$, there are two distinct sublattice magnetizations which result from the two different local fields [see Eq. (7b)]: the weak local field here is felt by the spins of the sublattices linked by η bonds; the magnetization of these sublattices undergoes a fall at the Ising transition temperature. Both sublattice magnetizations tend to zero at the KT transition temperature. In both cases ($\eta=1$ and 0.6), the sublattice magnetizations decrease slowly with increasing lattice size even at temperatures below the transitions. We have also observed the same behavior in the ferromagnetic XY spin systems. This may be a characteristic feature of 2D XY spin systems.

The spatial spin correlation functions G at given distance R and temperature T have been calculated by first averaging over the sample and then over the time, after equilibrating the system. G has the same features as the sublattice magnetizations: at a given distance, G decreases, though very slowly, with increasing lattice sizes [see Fig. 9(a)]. The distance dependence of G is shown in Fig. 9(b) for the fully frustrated case at various temperatures. For comparison, we have included here the curve $G(R)$ for the 2D ferromagnetic XY model at a temperature very close to the transition point. This curve is to be compared with that of the fully frustrated case at $T=0.45$. One observes a stronger decrease of $G(R)$ in the former case. This behavior is also seen in the ordered phase. However, in the disordered phase, the reverse is observed.

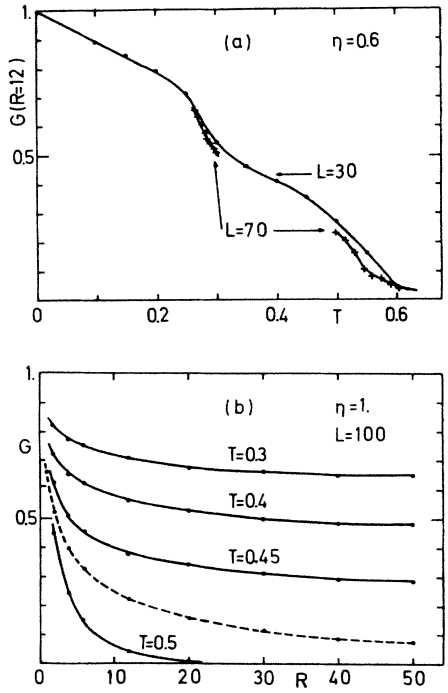

FIG. 9. Spatial spin correlation function G: (a) as a function of temperature at 12 lattice spacings for $\eta=0.6$, $L^2=30^2$ (solid circles) and 70^2 (crosses); (b) as a function of lattice spacing at various temperatures for $\eta=1$ and $L^2=100^2$. Dashed line is for ferromagnetic XY model ($\eta=1$) at a temperature close to transition point ($T=1$).

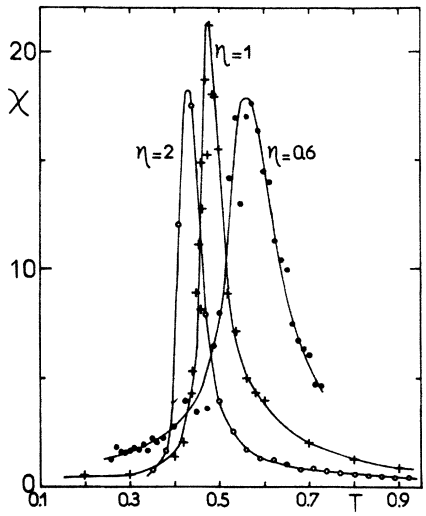

FIG. 10. Magnetic susceptibility χ calculated by magnetization fluctuations is shown as a function of T for typical values of η: 0.6 (solid circles), 1 (crosses), and 2 (open circles). Solid lines are guides to the eye ($L^2=30^2$).

E. Magnetic susceptibility

We have computed the magnetic susceptibility χ by calculating thermal fluctuations of the total magnetization defined in the same way as (12) but with the sum taken over the whole lattice. The results are shown in Fig. 10 as a function of temperature for typical values of η. For η rather far below 1, one observes a peak of χ at the KT-like transition but no peak at the Ising-like transition. In contrast, for η larger than 1, one observes only a sharp peak at the Ising-like transition. At present, we have no clear interpretation for the absence of the peak in χ at one of the transitions for $\eta\neq 1$. In the fully frustrated case ($\eta=1$), a sharp peak is observed at the transition as expected. The peak at the Ising-like transition in the case $\eta=2$ (Fig. 10) is very well fitted by a power law $\chi\propto|T-T_c|^{-\gamma}$ where T_c is the peak temperature. We find that $\gamma=1.2\pm0.1$, which is very small compared to that of the real 2D Ising lattice ($\gamma=\frac{7}{4}$). This may be due to the fact that the XY character (global rotation) cannot be completely excluded at the Ising-type transition in the model studied here. For $\eta=1$, we have fitted the peak of χ with both power law and XY exponential law $\chi\propto\exp(C/|T-T_c|^{1/2})$ where C is a constant. As it turns out, the power law fits much better than the exponential law, with the same value of γ as for $\eta=2$. This indicates once more the dominant Ising character of the transition in the fully frustrated case.

IV. SUMMARY AND CONCLUDING REMARKS

By introducing the frustration parameter η, we have been able to show how the single transition in Villain's fully frustrated lattice with XY spins results from the merging of two transitions, one of Ising type and the other of Kosterlitz-Thouless type. This sheds light on the nature of phase transitions in 2D uniformly frustrated XY spin systems which has not been clarified in previous work.[2,14–18] We have shown that the ground state is doubly degenerate for $\eta>\frac{1}{3}$. It is this double degeneracy that is responsible for the Ising-type transition observed at low temperature when $\eta\neq1$, in addition to a Kosterlitz-Thouless-type transition at higher temperature due to the continuous symmetry breaking. The nature of these transitions has been confirmed by finite-size-scaling analysis and visualization of ordering as well as by other MC data.

We note that there exists another uniformly frustrated model (see, e.g., Refs. 2, 17, and 18): varying the frustration results in changing the periodicity of canted ground-state spin configurations without changing the bond strength, in contrast to our model. Both models allow us to change the XY spin system for the ferromagnetic state to the fully frustrated one, but by two different pathways. However, the results from our model are more convincing as far as the high-temperature transition is concerned: the other model yields only a shoulder in the specific heat[22] while our model gives a more pronounced peak for this transition. Besides, Garel and Doniach[23] have also found for 2D XY helimagnet two transitions of Ising- and KT-type occurring at low and high temperatures, respectively, just as in our model. Finally, we suggest that our model might have an experimental realization such as a planar array of alternate rows of Josephson junctions of different coupling strengths, in transverse magnetic field.

Note added. After having submitted this work, we

learned that Granato and Kosterlitz[24] have obtained by a Landau-Ginzburg-Wilson analysis a phase diagram similar to ours (Fig. 7), using a coupled XY model which, they showed, is equivalent to the fully frustrated XY model in the vicinity of $\eta=1$.[25] Also, Choi and Stroud[26] have found a single transition for $\eta=1$, in agreement with our results.

ACKNOWLEDGMENTS

We wish to thank J. M. Kosterlitz for several stimulating discussions. Thanks are also due to D. Stroud and P. Viot for numerous valuable conservations and to G. Toulouse for bringing our attention to Ref. 17. Numerical calculations have been carried out on the Floating Point Systems array processor FPS-164 at Ecole Normale Supérieure. Computer time generously provided by Groupement de Recherches Coordonnées (GRECO) Expérimentation Numérique is gratefully acknowledged. Groupe de Physique des Solides de l'Ecole Normale Supérieure is Laboratoire associé au Centre National de la Recherche Scientifique. Laboratoire de Spectroscopie Hertzienne de l'Ecole Normale Supérieure is Unité associée au Centre National de la Recherche Scientifique.

*Permanent address: Laboratoire de Spectrométrie Physique, Université Scientifique et Médicale de Grenoble, Boîte Postale No. 68, 38042 Saint-Martin-d'Hères, France.

[1]G. Toulouse, Commun. Phys. **2**, 115 (1977).
[2]T. C. Halsey, J. Phys. C **18**, 2437 (1985).
[3]H. T. Diep, P. Lallemand, and O. Nagai, J. Phys. C **18**, 1067 (1985).
[4]K. Wada and T. Ishikawa, J. Phys. Soc. Jpn. **52**, 1774 (1983).
[5]D. Blankschtein, M. Ma, A. N. Berker, G. S. Grest, and C. M. Soukoulis, Phys. Rev. B **29**, 5250 (1984).
[6]M. D. Phani, J. Lebowitz, and M. Kalos, Phys. Rev. B **21**, 4027 (1980).
[7]T. L. Polgreen, Phys. Rev. B **29**, 1468 (1984).
[8]O. Nagai, Y. Yamada, and H. T. Diep, Phys. Rev. B **32**, 480 (1985).
[9]H. T. Diep, A. Ghazali, and P. Lallemand, J. Phys. C **18**, 5881 (1985).
[10]P. Lallemand, H. T. Diep, A. Ghazali, and G. Toulouse, J. Phys. Lett. (Paris) **46**, L1087 (1985).
[11]J. Villain, J. Phys. C **10**, 1717 (1977).
[12]G. Wannier, Phys. Rev. **79**, 357 (1950); Phys. Rev. B **27**, 5017 (1973).
[13]O. Nagai, M. Toyonaga, and H. T. Diep, J. Magn. Magn. Mater. **31-34**, 1313 (1983).
[14]S. Teitel and C. Jayaprakash, Phys. Rev. B **27**, 598 (1983).
[15]S. Miyashita and H. Shiba, J. Phys. Soc. Jpn. **53**, 1145 (1984).
[16]D. H. Lee, J. D. Joannopoulos, J. W. Negele, and D. P. Landau, Phys. Rev. Lett. **52**, 433 (1984).
[17]M. Yosefin and E. Domany, Phys. Rev. B **32**, 1778 (1985).
[18]M. Y. Choi and S. Doniach, Phys. Rev. B **31**, 4516 (1985).
[19]J. M. Kosterlitz and D. J. Thouless, J. Phys. C **6**, 1181 (1973); J. M. Kosterlitz, *ibid.* **7**, 1046 (1974).
[20]J. Tobochnik and G. V. Chester, Phys. Rev. B **20**, 3761 (1979).
[21]J. E. Van Himbergen and S. Chakravarty, Phys. Rev. B **23**, 359 (1981).
[22]W. Y. Shih and D. Stroud, Phys. Rev. B **30**, 6774 (1984); T. C. Halsey (unpublished).
[23]T. Garel and S. Doniach, J. Phys. C **13**, L887 (1980).
[24]E. Granato and J. M. Kosterlitz (private communication).
[25]E. Granato and J. M. Kosterlitz, J. Phys. C **19**, L59 (1986).
[26]M. Y. Choi and D. Stroud, Phys. Rev. B **32**, 5773 (1985).